

# Berry-curvatures and the anomalous Hall effect in Heusler compounds

Jürgen Kübler<sup>1</sup> and Claudia Felser<sup>2</sup>

<sup>1</sup>*Institut für Festkörperphysik, Technische Universität Darmstadt, 64289 Darmstadt, Germany,*

<sup>2</sup>*Institut für Anorganische Chemie und Analytische Chemie,  
Johannes Gutenberg - Universität, 55099 Mainz\**

(Dated: October 14, 2011)

Berry curvatures are computed for a set of Heusler compounds using density functional (DF) calculations and the wave functions that DF provide. The anomalous Hall conductivity is obtained from the Berry curvatures. It is compared with experimental values in the case of Co<sub>2</sub>CrAl and Co<sub>2</sub>MnAl. A notable trend cannot be seen but the range of values is quite enormous. The results for the anomalous Hall conductivities and their large variations can be qualitatively understood by means of the band structure and the Fermi-surface topology.

PACS numbers: 75.10.Lp, 75.47.Np, 75.70.Tj

Keywords: Berry curvature, Hall effect, Half-metallic ferromagnets, Heusler compounds

A rather recent discovery is that the Berry-curvature supplies an additional term to the electron velocity in a crystal [1]. It is an important correction to all transport properties that rely on the velocity, in particular, it describes the leading contribution to the anomalous Hall effect [2].

Heusler compounds, especially those based on Co, with their regularities in many physical properties, like the Slater-Pauling behavior [3], invite the question if such regularities are also present in the anomalous Hall effect (AHE). This is one of the questions we turn to here. Furthermore, a considerable number of Heusler compounds are half-metallic ferromagnets, *i.e.* they are gapped in one spin channel; therefore, in notable applications one tries to make use of spin currents, for which our calculations can serve as guide lines in estimates of the degree of spin polarization of the current.

The Berry curvature follows from the Berry vector,

$$\mathcal{A}(\mathbf{k}) = i \sum_n \langle u_{\mathbf{k},n} | \nabla_{\mathbf{k}} | u_{\mathbf{k},n} \rangle, \quad (1)$$

where  $u_{\mathbf{k},n}(\mathbf{r})$  is the crystal-periodic eigenfunction having wave vector  $\mathbf{k}$  and band index  $n$ . The sum extends over the occupied states which for metals vary with  $\mathbf{k}$ . The Berry curvature is written as

$$\Omega(\mathbf{k}) = \nabla_{\mathbf{k}} \times \mathcal{A}(\mathbf{k}). \quad (2)$$

The Berry curvature can be calculated in different ways. The common procedure is via a Kubo-like approach, where one calculates essentially a Green's function, see e.g. ref. [4]. The other, less common approach, is via the wave-functions directly. The numerical treatment used here to calculate  $\Omega$  is basically a finite-difference approach, some details may be summarized using the references [5–8] as follows. One begins by computing the so-called link-variable [5]

$$U_{\mathbf{j}}(\mathbf{k}) = \det[\langle u_{\mathbf{n}\mathbf{k}} | u_{\mathbf{m}\mathbf{k}+\mathbf{j}} \rangle], \quad (3)$$

where the determinant is evaluated for the occupied states  $n$  and  $m$ . The component of  $\mathcal{A}(\mathbf{k})$  along  $\mathbf{j}$  is then

$$\mathcal{A}_{\mathbf{j}}(\mathbf{k}) = \text{Im} \log U_{\mathbf{j}}(\mathbf{k}), \quad (4)$$

which yields by finite differences for the  $z$ -component of the Berry curvature (except for a scaling factor)

$$\Omega_z(\mathbf{k}) = \text{Im} \log \frac{U_y(\mathbf{k} + \hat{\mathbf{k}}_x) U_x(\mathbf{k})}{U_y(\mathbf{k}) U_x(\mathbf{k} + \hat{\mathbf{k}}_y)}. \quad (5)$$

The logarithm implies that the results are mod  $2\pi$ .

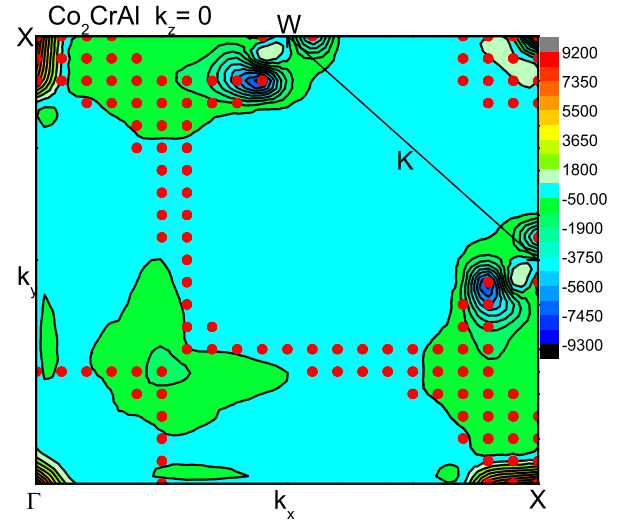


FIG. 1: The Berry-curvature in the  $k_z=0$  plane for Co<sub>2</sub>CrAl. The color codes are in units of  $(\Omega\text{cm})^{-1}$ . The labels follow the standard notation for the face-centered-cubic crystal. The red dots mark band energies of majority-spin electrons within 40 meV below the Fermi energy.

The Heusler compounds of interest here are face-centered cubic possessing the  $L_{21}$  symmetry, except for

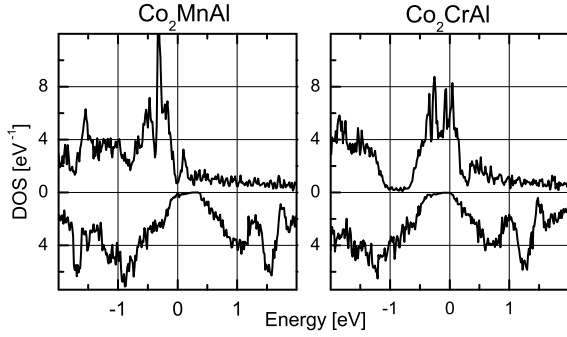


FIG. 2: Density of states of  $\text{Co}_2\text{MnAl}$  and  $\text{Co}_2\text{CrAl}$ . The upper parts of the figures describe majority-spin electrons the lower parts minority-spin electrons. In contrast to spin up and down, these terms are well defined even in the spin-orbit coupled systems.

$\text{Mn}_2\text{PtSn}$  which is tetragonal with space-group No. 119. They are ferromagnetic; time-reversal symmetry is therefore broken which leads to a non-zero Berry curvature [1, 2].

The wave functions are calculated in the local density-functional approximation (LDA) [9] using the ASW method [10]. Spin-orbit coupling (SOC), which is essential for this theory, is included in a second variation [11].

The anomalous Hall conductivity,  $\sigma_{xy}$ , is given by the Berry curvature as

$$\sigma_{xy} = -\frac{e^2}{h} \frac{1}{N} \sum_{\mathbf{k} \in (\text{BZ})} \Omega_z(\mathbf{k}) f(\mathbf{k}), \quad (6)$$

where  $f(\mathbf{k})$  is the Fermi distribution function,  $\Omega_z(\mathbf{k})$  is the  $z$ -component of the berry curvature for the wave-vector  $\mathbf{k}$ ,  $N$  is the number of electrons in the crystal and the sum extends over the Brillouin zone (BZ).

In the figures to be presented the  $z$ -component of the Berry-curvature is shown in a cut through the fcc Brillouin (BZ) Zone; this was chosen to be the  $k_z=0$  plane. While the number of  $k$ -points (441) to obtain these figures could be chosen sufficiently large for the plots to show significant details, the Hall conductivity,  $\sigma_{xy}$ , at  $T = 0$  K which was calculated by means of Eq. (6) needed very large numbers of  $k$ -points for convergence. Our results are converged to within about 20 % with about 2000 points in the irreducible wedge of the BZ.

Haldane [12] showed that Fermi-liquid theory is still valid even though it appears that the Hall conductivity, Eq. (6), depends on all states below the Fermi energy. He showed that the Berry curvature can be transformed to the Berry phase on the Fermi-surface only. Thus an alternative to our calculations exists [2]. This is a transformation to Berry phases on the Fermi-surface, but it requires good software to handle the three dimensional surfaces.

Our calculations, in contrast, are indeed quite straight forward. The results of our calculations are collected in Table. I, where also an estimate,  $P$ , of the degree of spin-polarization of the Hall current is given. This is obtained by counting the number of majority-spin electron states within 40 meV below the Fermi energy,  $N^+$ , in the irreducible wedge of the BZ, and similarly the number of minority-spin states,  $N^-$ , then  $P = N^+/(N^+ + N^-)$ . These numbers are given by  $N^\pm = \sum_{\mathbf{k}} n^\pm(\mathbf{k})$ , where the spin-resolved norms,  $n^\pm(\mathbf{k})$ , are either 0 or 1, but SOC mixes into a given spin state contributions of the opposite spin, thus a "spin filter" finds the  $n^\pm(\mathbf{k})$  larger than 0 or smaller than 1.

TABLE I: Collection of experimental and calculated data relevant for the Hall conductivity.  $N_V$  is the number of valence electrons,  $M^{\text{exp}}$  is the the experimental and  $M^{\text{calc}}$  the calculated magnetic moment in  $\mu_B$ ,  $\sigma_{xy}$  is the Hall conductivity in  $(\Omega\text{cm})^{-1}$ , calculated by means of eq.(6),  $P$  is an estimate of the spin polarization of the Hall current.

Compound	$N_V$	$M^{\text{exp}}$	$M^{\text{calc}}$	$\sigma_{xy}$	$P$ (%)
$\text{Co}_2\text{VGa}$	26	1.92	1.953	66	65
$\text{Co}_2\text{CrAl}$	27	1.7	2.998	438	100
$\text{Co}_2\text{VSn}$	27	1.21	1.778	-1489	35
$\text{Co}_2\text{MnAl}$	28	4.04	4.045	1800	75
$\text{Rh}_2\text{MnAl}^{(1)}$	28	—	4.066	1500	94
$\text{Mn}_2\text{PtSn}^{(2)}$	28	—	6.66	1108	91
$\text{Co}_2\text{MnSn}$	29	5.08	5.00	118	82
$\text{Co}_2\text{MnSi}$	29	4.90	4.98	228	100

<sup>(1)</sup> Crystal data from Pearson's Crystal Data.

<sup>(2)</sup> Crystal data from J. Winterlik (private communication).

Starting with the valence electron number  $N_V=26$ , the Hall conductivity is calculated for  $\text{Co}_2\text{VGa}$  and is given in Table I. The Berry curvature for  $\text{Co}_2\text{CrAl}$  with  $N_V=27$  valence electrons is shown in Fig.1 and the integrated value is given in Table I. All states within 40 meV below the Fermi energy are majority-spin states (red dots in the figure) which agrees with the value of  $P$  given in the Table. The density of states of  $\text{Co}_2\text{CrAl}$  shown in Fig.2 also agrees with  $P = 100\%$ . There is an experimental value of  $\sigma_{xy} = 125 (\Omega\text{cm})^{-1}$  to be compared with our value of  $\sigma_{xy} = 472 (\Omega\text{cm})^{-1}$ . The difference is significant, but the rather low value measured for the magnetic moment of  $1.7 \mu_B$  cannot be explained by our density of states shown in fig. (2) which results in a magnetic moment of  $3 \mu_B$ . The reason is most likely that the sample is disordered and does not have the ideal Heusler  $L_{21}$  crystal structure. Furthermore, it is possible but less likely that the other contributions to the Hall effect, *i.e.* side jump-and skew scattering-mechanisms, contribute considerably.

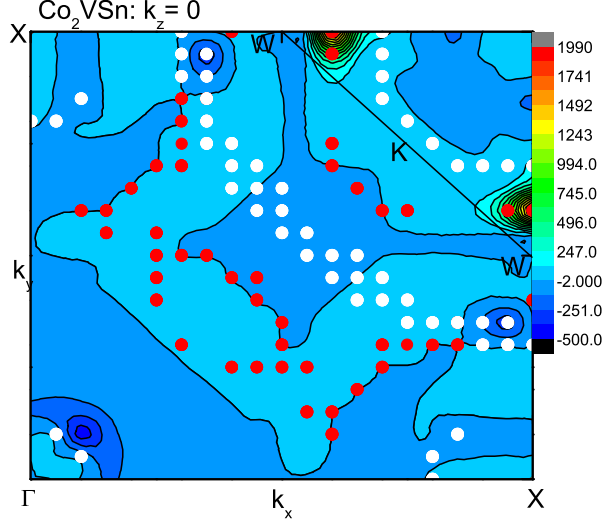


FIG. 3: The Berry-curvature in the  $k_z=0$  plane for  $\text{Co}_2\text{VSn}$ . Color code and labels as in Fig. 1. The red and white dots mark band energies of majority-spin and minority-spin electrons, respectively, within 40 meV below the Fermi energy.

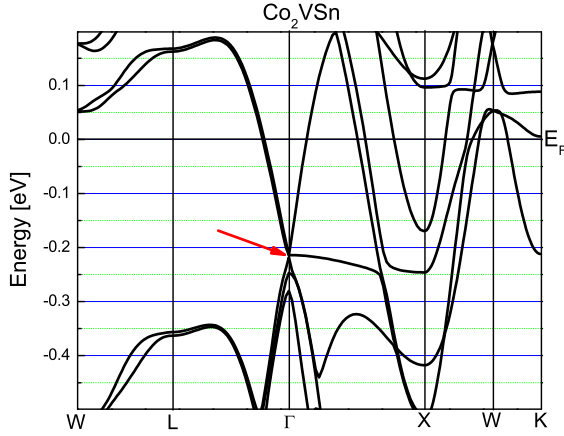


FIG. 4: Band structure near the Fermi edge of  $\text{Co}_2\text{VSn}$ . The red arrow points toward the Dirac point.

The Heusler compound  $\text{Co}_2\text{VSn}$  also with  $N_V=27$  valence electrons is not a half-metallic ferromagnet [3] having a measured moment of  $1.21 \mu_B$  and a calculated one of  $1.78 \mu_B$ . In Fig.3 we show the Berry curvature in the  $k_z = 0$  plane as before. The band-structure reveals in Fig.4 a Dirac-cone below the Fermi energy describing minority-spin electrons. They show up in the berry curvature as the semi circle and the white dots around

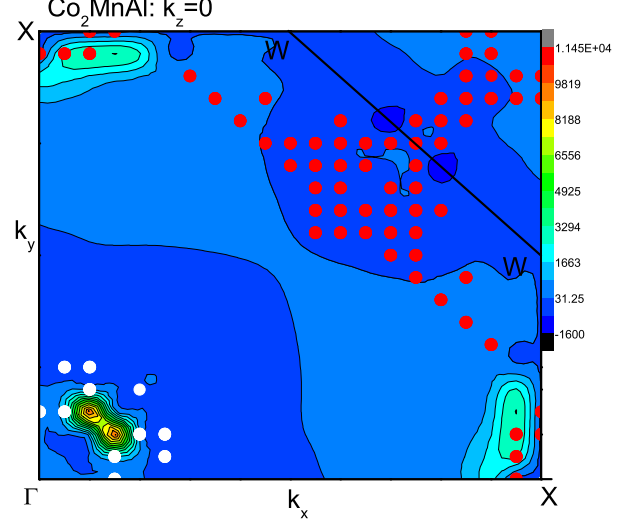


FIG. 5: The Berry-curvature in the  $k_z=0$  plane for  $\text{Co}_2\text{MnAl}$ . Color code, labels and dots as in Fig.3.

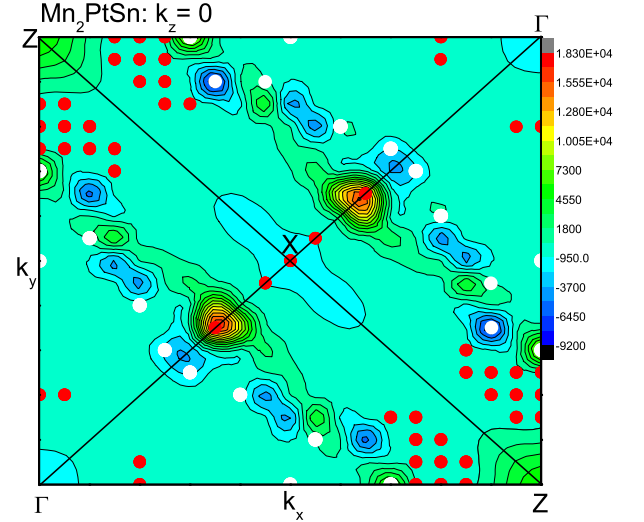


FIG. 6: The Berry-curvature in the  $k_z=0$  plane for  $\text{Mn}_2\text{PtSn}$ . Color code and dots as in Fig. 3. The symmetry labels are the standard ones for the bct lattice.

the  $\Gamma$ -point. The states seen near the  $W$ -points are due to majority-spin electrons (red dots). The Dirac cone results in a large negative contribution to the Hall conductivity, while the other states give less positive contributions resulting in a calculated Hall conductivity of  $\sigma_{xy} = -1489 (\Omega\text{cm})^{-1}$  and a polarization of only 35 %.

Next is Fig.5 for  $\text{Co}_2\text{MnAl}$  with 28 valence electrons.

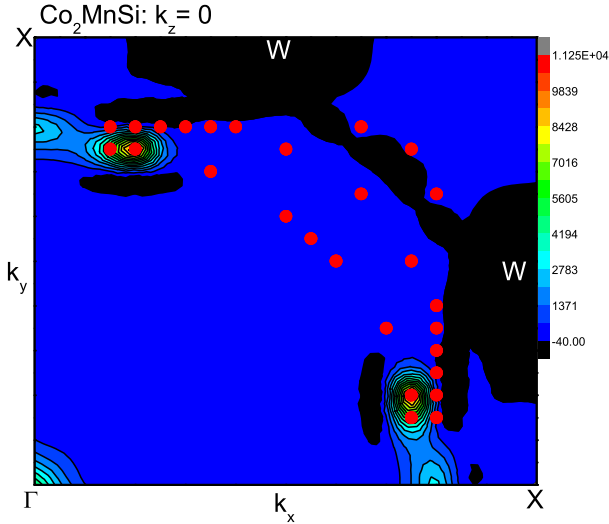


FIG. 7: The Berry-curvature in the  $k_z=0$  plane for  $\text{Co}_2\text{MnSi}$ . Color code, labels and dots as in Fig.3.

The magnetic moment is measured and calculated to be  $4.04 \mu_B$ . Here we obtain the startling high value of  $\sigma_{xy} = 1800 (\Omega\text{cm})^{-1}$ . In the density of states, Fig. 2, the Fermi energy sits in tails of states at the low-energy side of the gap, therefore we see down-spin electrons in the Fermi surface near  $\Gamma$  and up-spin electrons near  $X$  (red dots). Both contribute positive to  $\sigma_{xy}$ , while negative contributions originate from states around  $K$  and  $W$ . The Fermi surface near  $\Gamma$  shows up in Fig.5 as two small imperfectly resolved circles and the white dots.

There is a recent study of the AHE for  $\text{Co}_2\text{MnAl}$  by Vidal *et al.* [14] which allows a rough estimate of the Hall conductivity. If one takes their measured saturation value of the Hall resistivity of  $\rho_{xy} = 20 \mu\Omega\text{cm}$  and their estimated specific resistivity of order of  $100 \mu\Omega\text{cm}$  then the Hall conductivity is obtained to be approximately  $2000 (\Omega\text{cm})^{-1}$ . This could be called to be in good agreement with the theory were it not for experimentally disordered Mn and Al sites in the samples a fact that is stressed by Vidal *et al.* [14].

To guide the search for other ferromagnetic compounds with a large Hall conductivity we enquired into the role of the strength of SOC. For this reason we increased the SOC strength by 40% and found for  $\text{Co}_2\text{MnAl}$  a conductivity of  $\sigma_{xy} = 2150 (\Omega\text{cm})^{-1}$ . This increase originates from the states near  $X$  in Fig.5 and from a diminishing importance of the states near  $K$ . The increased role of SOC is realized in  $\text{Rh}_2\text{MnAl}$ , for which, therefore, the Hall conductivity was calculated and found to be  $1500 (\Omega\text{cm})^{-1}$ . This is within the value obtained for  $\text{Co}_2\text{MnAl}$  but does not show the expected increase.

Since it is the valence electron number of  $N_V = 28$  where the conductivity is especially large, we calculated the electronic structure of the tetragonal Heusler compound  $\text{Mn}_2\text{PtSn}$  which also has 28 valence electrons. The Berry curvature is shown in Fig.6, see also Table I. It is seen that the minority-spin states result in negative contributions to the Hall conductivity, the total  $\sigma_{xy} = 1108 (\Omega\text{cm})^{-1}$  being only reasonably large.

For  $\text{Co}_2\text{MnSi}$ , finally, the Berry curvature is shown Fig. 7. This compound has 29 valence electrons, it is a half-metallic ferromagnet having a measured magnetic moment of  $4.90 \mu_B$  which is calculated to be  $4.98 \mu_B$ . The spin-polarization of the Hall current is 100 %, still, the Hall conductivity is only  $\sigma_{xy} = 228 (\Omega\text{cm})^{-1}$ .

Summarizing we state that the strong trends like the Slater-Pauling behavior are not seen in the Hall conductivity. However, large values of the Hall conductivity can be found in special cases like  $\text{Co}_2\text{MnAl}$  and other systems having 28 valence electrons. The strength of SOC is shown to be but one ingredient to ensure large values of  $\sigma_{xy}$ , however, a general rule still has to be found.

The generous supply of computer time by U. Nowak (Universität Konstanz) and the financial support by the DFG/ASPIMATT project (unit 1.2-A) are gratefully acknowledged.

---

\* Electronic address: jkubler@fkp.tu-darmstadt.de

- [1] Di Xiao, Che Chang, and Qian Niu: *Rev. Mod. Phys.* **82**, 1959 (2010)
- [2] N. Nagaosa, J. Sinova, S. Onoda, A.H. MacDonald, and N.P. Ong: *Rev. Mod. Phys.* **82**, 1539 (2010)
- [3] J. Kübler, G.H. Fecher, and C. Felser: *Phys. Rev. B* **76**, 024414 (2007)
- [4] Y. Yao, L. Kleinman, A.H. MacDonald, J. Sinova, T. Jungwirth, D. Wang, E. Wang, and Q. Niu: *Phys. Rev. Lett.* **92**, 9037204 (2004)
- [5] T. Fukui and Y. Hatsugai: *J. Phys. Soc. Jpn.* **76**, 053702 (2007)
- [6] R.D. King-Smith and D. Vanderbilt: *Phys. Rev. B* **47**, 1651 (1993)
- [7] R. Resta: *Rev. Mod. Phys.* **66**, 899 (1994)
- [8] D. Xiao, Y. Yao, W. Feng, J. Wen, W. Zhu, X.-Q. Chen, G. M. Stocks, and Z. Zhang: *Phys. Rev. Lett.* **105**, 096404 (2010)
- [9] W. Kohn and L.J. Sham: *Phys. Rev.* **140**, A1133 (1965)
- [10] A.R. Williams, J. Kübler, and C.D. Gelatt: *Phys. Rev. B* **19**, 6094 (1979)
- [11] A.H. MacDonald, W.E. Pickett, and D.D. Koelling: *J. Phys. C.: Sol. State Phys* **13**, 2675 (1980)
- [12] F.D.M. Haldane: *Phys. Rev. Lett.* **93**, 206602 (2004)
- [13] A. Husemann and L.J. Singh: *Phys. Rev. B* **73**, 172917 (2006)
- [14] E.V. Vidal, G.Stryganyuk, H. Schneider, C. Felser, and G. Jakob: *Appl. Phys. Lett.* **99**, 132509 (2011)